A Note on Numerical Solution of Classical Darboux Problem

K. Harish Kumar*[1] and Ram Jiwari

Department of Mathematics, Indian Institute of Technology Roorkee, Roorkee - 247667, India

Abstract

Recently, many authors studied the numerical solution of the classical Darboux problem in its integral form via a two-dimensional nonlinear Volterra-Fredholm integral equation. In the present article, a numerical technique based on the Chebyshev wavelet is proposed to solve the Darboux problem directly without converting into a nonlinear Volterra-Fredholm integral equation. The proposed technique is different from the techniques discussed in [1, 2, 4, 7, 11, 16, 17, 18, 19]. The proposed approach produces higher accuracy than its counterpart techniques. The proposed scheme illustrated with suitable examples to show the advantages in-terms of its accuracy with lesser grid size.

Keywords: Chebyshev wavelet, Collocation Method, Darboux problem, Hyperbolic partial differential equation, Quasilinearization.

1. Introduction

In the present article, a Chebyshev wavelet based numerical scheme proposed for solving the classical Darboux problem, a fundamental problem in mathematical physics

$$\frac{\partial^2 v}{\partial \zeta \partial t} = g(\zeta, t, u), \quad \zeta, t \in [0, 1] \tag{1.1}$$

[1]harish296228@gmail.com, Tel. No. +91-8109112193

with the initial condition $u(\zeta, 0) = f_1(\zeta)$ and the boundary condition $u(0, t) = f_2(t)$, where $f_1(\zeta)$ and $f_2(t)$ are differentiable functions with $f_1(0) = f_2(0)$. The choice $g(\zeta, t, v) = \sin v$, in Eqn (1.1) leads to the well known Darboux problem for the Sine Gordon equation [21]. Eqn (1.1) is nothing but the nonlinear Voltera-Fredholm integral equation in its characteristic form. Sometimes it is named as Goursat problem. Eq (1.1) plays an important role in various mathematical model such as condensed matter physics, fluid flow, nonlinear optics, radiation theory, solid and high energy physics, quantum mechanics. A detailed literature survey and applications of Darboux problem can be found in [8]. Recently many authors [2, 4, 16, 11, 1, 19, 17, 18] produced the numerical solution of classical Darboux problem by solving the following equivalent two dimensional Voltera-Fredholm integral equation

$$v(\zeta, t) = f_1(\zeta) + f_2(t) - f_1(0) + \int_0^{\zeta} \int_0^{t} g(s, s', u) \mathrm{d}s \mathrm{d}s' \quad \zeta, t \in [0, 1] \tag{1.2}$$

Various numerical methods developed to handle (1.2) in recent literature. Among them Cubature method [12], Haar wavelet method [4], hybrid of block pulse functions and Taylor series [16], iterative method based on Newton-Cotes method, Legendre polynomial [18], operational Tau method [11], moving least square approximation [1], radial basis function [2, 8, 23], spectral Galerkin method [17], Successive iterative approach [7] and two dimensional differential transform method [19] are some of the modern techniques. Few researchers [8, 12] solved the Darboux problem (1.1) as it is instead of solving its equivalent two-dimensional Volterra-Fredholm integral equation (1.2). Though the existing methods obtain the accuracy with decent grid size, in the present paper a new method based on Chebyshev wavelet is proposed to solve (1.1) which is an equivalent form of (1.2). The highlights of the proposed work as follows.

- The Darboux problem (1.1) in its differential equation form is solved instead of solving its integro-differential form (1.2).

- The major advantage is that in the present method the final resultant matrix is very simple.

- There is no involvement of kernel in the proposed method (CWM) unlike in the methods [1, 2, 4, 7, 11, 16, 17, 18, 19].

Recently, various wavelet-based numerical techniques are successfully applied to solve differential equations [3, 13, 14, 20] very few researchers have used Chebyshev wavelets [5, 15, 22] for solving different types of differential equations. In this paper, the Chebyshev wavelet-based numerical scheme is developed for the Darboux problem without converting the Eqn (1.1) into the equivalent integral Eqn (1.2).

The rest of the paper is organized as follows. The basic ideas on Chebyshev wavelet quasilinearization for the Darboux problem are provided in Section 2. Section 3 details the numerical implementations of the Chebyshev wavelet collocation method for problem (1.1). In Section 4 various examples are solved for different choices of $f_1(\zeta)$ and $f_2(t)$. The obtained results are also compared with the exact solution and other numerical methods. The discussions are concluded in Section 5 by stating the various merits of the proposed scheme and possible future enhancements.

2. Chebyshev Wavelet collocation method

Recently, Chebyshev wavelet operational matrix methods are used to solve differential equations namely, integral type equations [6], ordinary type differential equations [9] and partial type differential equations [10]. The Chebyshev wavelets family is defined by:

$$\psi_{m,n}(\zeta) = \begin{cases} \frac{2^{\frac{k}{2}}\alpha_m}{\sqrt{\pi}} T_m(2^k\zeta - \hat{n}) \quad for\ \zeta\ \in [\frac{\hat{n}-1}{2^k}, \frac{\hat{n}+1}{2^k}) \\ 0, \quad \text{otherwise,}. \end{cases} \tag{2.1}$$

where

$$\alpha_m = \begin{cases} 1 \text{ for } m = 0 \\ \sqrt{2}, \quad m > 0. \end{cases} \tag{2.2}$$

where $m, n, k \in \mathbb{N}$, $n = 1, 2, \ldots 2^{k-1}$, and $\hat{n} = 2n - 1$. To find the Chebyshev polynomials, the following well-acquainted recurrence relation used. For $m = 1, 2, 3 \cdots$

$$T_0(\zeta) = 1, \quad T_1(\zeta) = \zeta \tag{2.3}$$

$$T_{m+1}(\zeta) = 2\zeta T_m(\zeta) - T_{m-1}(\zeta) \tag{2.4}$$

The simplified equivalent version of (2.1) is given below:

$$\psi_i(\zeta) = \begin{cases} \frac{2^{\frac{k}{2}}\alpha_m}{\sqrt{\pi}} T_m(2^k\zeta - \hat{n}) & \text{if } \zeta \in [\frac{\hat{n}-1}{2^k}, \frac{\hat{n}+1}{2^k}) \\ 0 & \text{otherwise.} \end{cases} \tag{2.5}$$

where $n = 1, 2, \cdots 2^{k-1}$, $m = 0, 1, 2, \cdots$ and $i = n + 2^{k-1}m$. The orthogonal property of Chebyshev polynomial guaranty that the Chebyshev wavelets family form an orthogonal set in $L^2(0, 1)$. Consequently, it forms an orthonormal basis for $L^2(0, 1)$.

3. Numerical Implementation

Quasilinearization scheme for Darboux problem (1.1) is as follows

$$\frac{\partial^2 v_{n+1}}{\partial\zeta\partial t} = g(v_n, \zeta, t) + \frac{\partial g}{\partial v_n}(v_{n+1} - v_n) \quad n = 0, 1, 2 \cdots \tag{3.1}$$

with initial conditions $u_{n+1}(\zeta, 0) = f_1(\zeta)$, $u_{n+1}(0, t) = f_2(t)$, $0 \leq \zeta \leq 1$.Let A^T denotes transpose of the matrix A. The highest derivatives in the differential equation can be can be approximated as

$$\frac{\partial^2 v_{n+1}}{\partial\zeta\partial t} = \sum_{i=1}^{N_1}\sum_{j=1}^{N_1} a_{i,j}^{n+1}\psi_i(\zeta)\psi_j(t) = \Psi^T(t)A^{n+1}\Psi(\zeta) \tag{3.2}$$

where $A^{n+1} = [a_{i,j}^{n+1}]$, $\Psi(\zeta) = [\psi_i(\zeta)]^T$ and $\Psi(t) = [\psi_j(t)]^T$ for $1 \leq i, j \leq N_1$. From (3.2) one can get $v^{n+1}(\zeta, t)$ and it can be represented as follows.

$$v^{n+1}(\zeta, t) = \Psi^T(t)(P^T)A^{n+1}P\Psi(\zeta) + v^{n+1}(\zeta, 0) + v^{n+1}(0, t) - v^{n+1}(0, 0) \quad (3.3)$$

where P is the operational matrix for integration discussed in [5]. After using the set of collocation points $\{(\zeta_i, t_j) : \zeta_i = t_i = \frac{i-0.5}{N_1}, 1 \leq i, j \leq N_1\}$, the equation (3.3) can be written as

$$v_{n+1}(\zeta, t) \;\; = \;\; P_1^T A^{n+1} P_1 + S_1 + S_2 - S_3 \quad (3.4)$$

where $S_1 = [u(\zeta_i, 0)]$, $S_2 = [u(0, t_j)]$, $S_3 = [u(0, 0)]$, $A^{n+1} = [a_{i,j}]$ and $P_1 = P\Psi(t_j)$. The equation (3.1) can be written as

$$\phi^T A^{n+1}\phi - S_4 \circ (P_1^T A^{n+1} P_1) \;\; = \;\; S_6 \quad (3.5)$$

where $\phi = [\Psi^T(\zeta_i)] = [\Psi^T(t_j)]$, $S_4 = [\frac{\partial g(v_n(\zeta_i,t_j),\zeta_i,t_j)}{\partial v_n}]$, $S_5 = [v_n(\zeta_i, t_j)]$ and $S_6 = S_5 + S_4 \circ (S_1 + S_2 + S_3)$. At each step, the above equation contains one unknown matrix with one equation which needs to be solved. Initially above equation needs to be solved for v_1 by taking initial guess v_0 by bringing the equation (3.5) into $L_1\theta_1 = b_1$ with the help of vectorization. Where $\theta_1 = [\text{vect}(A^{n+1})]'$ and $b_1 = [\text{vect}(S_6)]'$ and

$$L = \left[\; \phi^T \otimes \phi^T - (S_7) \times (P_1^T \otimes P_1^T) \; \right]$$

"vect" is the vectorization of a matrix [15, 22], $\otimes$ represents the Kronecker product between matrices and S_7 is diagonal matrix contains elements of S_4 at its diagonal position [15, 22]. Then the numerical solution of the Darboux problem can be obtained by stooping this iterative procedure with suitable stopping criteria. In the present method, the stopping criteria is used as $||v_{n+1} - v_n||_\infty \leq 10^{-08}$. The Darboux problem solution can be obtained from (3.4).

4. Numerical Example

The propose Chebyshev wavelet method (CWM) is tested for Darboux problem with various choices of $f_1(\zeta)$, $f_2(t)$ and $g(v, \zeta, t)$ as discussed in [1, 2, 4, 7, 8, 11, 12, 16, 17, 18, 19]. The performance of CWM is compared in terms of accuracy. Henceforth, the notation N_1 represents the number of Chebyshev wavelets. Initial guess $u_0 = 0$ is taken into consideration for all the discussed problems.

Example 4.1.

Consider the nonlinear Darboux problem discussed in [4, 17, 18]

$$\frac{\partial^2 v}{\partial \zeta \partial t} = v^2 - \zeta^4 - t^4 - 2\zeta^2 t^2. \tag{4.1}$$

with the initial conditions as $v(\zeta, 0) = u(0, t) = 0$ and the exact solution [18] is given as $v(\zeta, t) = \zeta^2 + t^2$. This equation is solved numerically using Chebyshev polynomial [17], Haar functions method [4] and Legendre polynomial method [17, 18]. The numerical results obtained using the quasilinearization based wavelet method is compared with Haar functions method [4] and Legendre polynomial method [18]. Table 1 and 2 shows that the proposed method based on wavelets performs extremely better than all the methods in [4, 17, 18]. For an instance from Table 1, the better error obtained using Haar functions methods [4] is $1.6e^{-04}$ for the grid size of 32×32 where as the present method gives an error of 0.0 for the same point with a grid size of 2×2. From Table 2 the advantage of Chebyshev wavelet based methods over chebyshev polynomial based methods [17] in-terms of accuracy can be observed clearly. Figure 5 gives the plot between $r = \frac{||v_{n+1} - v_e||_\infty}{||v_n - v_e||_\infty^2}$ and number of iterations which proves the quadratic convergence of the given scheme where v_e is the exact solution.

Example 4.2.

Consider the nonlinear Darboux problem discussed in [1, 2, 19]

$$\frac{\partial^2 v}{\partial \zeta \partial t} = (\zeta^2 + e^{-2t})u^2 + 2\zeta e^t - \zeta^4(1 + \zeta^2 e^{2t}). \tag{4.2}$$

with the initial conditions as $v(\zeta, 0) = \zeta^2$ and $v(0, t) = 0$ and the exact solution [19] is given as $v(\zeta, t) = \zeta^2 e^t$. This equation is solved numerically using Differential transform method [19], different types of weight function [1] and radial basis function [2]. The numerical results obtained using the quasilinearization based wavelet method are compared with Differential transform method [19], Gaussian weight function [1], Radial basis function [2] and Spline weight function [1] methods. Table 3 and 4 show that the proposed iterative methods based on wavelets performs extremely better than the method in [1, 19]. Figure 2 represents the CWM solution of the problem.

Example 4.3.

Consider the generalized non linear Darboux problem [4, 7, 11, 16]

$$\frac{\partial^2 v}{\partial \zeta \partial t} = (\zeta^3 + \cos t)u^2 + g(\zeta, t). \tag{4.3}$$

with the initial conditions as $v(\zeta, 0) = v(0, t) = 0$ and $g(\zeta, t) = \cos t - (\zeta^3 + \cos t)(\zeta \sin t)^2$. The exact solution is $v(\zeta, t) = \zeta \sin t$. The problem is already solved by different methods using Haar functions [4], Hybrid block pulse functions [16], Legendre base method [11] and Successive iterative approach [7]. Table 5, 6 and 7 presents the absolute errors and comparison between the proposed scheme and the existing methods in the literature. The proposed method outperforms the exiting methods in-terms of accuracy. Figure 3 represents the numerical solution (CWM) of the problem.

Example 4.4.

Consider the generalized non linear Darboux problem [8, 12].

$$\frac{\partial^2 v}{\partial \zeta \partial t} = e^{2v}. \tag{4.4}$$

with the initial conditions as $v(\zeta, 0) = \frac{\zeta}{2} - \log(e^{\zeta})$, $v(0, t) = \frac{t}{2} - \log(e^{t})$. The exact solution is $v(\zeta, t) = \frac{\zeta + t}{2} - \log \frac{e^{\zeta} + e^{t}}{2}$. Above problem is numerically solved using Cubature method [12] and Radial basis functions [8]. Table 8 gives the comparison between the proposed method and the existing methods [8, 12]. From Table 8 one can observe that better solution is obtained with just grid size of 10×10. Figure 3 represents the numerical solution (CWM) of the problem.

Example 4.5.

Now we will consider an example with unknown solution and stronger non-linearity. Consider the Sine-Gordon Darbous problem

$$\frac{\partial^2 v}{\partial \zeta \partial t} = \sin v \tag{4.5}$$

with the initial boundary condition as $v(x, 0) = \cos \zeta, v(0, t) = \cos t$. The numerical solution is obtained for different points in Table 9 with different grid sizes. Figure 4 represents the numerical solution (CWM) of the problem.

5. Conclusions

In the proposed work, the quasilinearization based Chebyshev wavelet method is discussed for the Darboux problem. To show the advantage of the proposed method, various types of numerical examples are provided including the Darboux problem for the Sine Gordon type of equation. The present approach is based on Chebyshev wavelet and handle the classical Darboux problem in its partial differential equation form. The proposed approach produces higher accuracy than its counterpart techniques. The proposed scheme illustrated with suitable examples

to show the advantages in terms of its accuracy with lesser grid size. The extension of the proposed technique to a higher dimension is simple and straight forward.

Acknowledgment: The first author K Harish Kumar would like to acknowledge the Department of Science and Technology (DST), New Delhi for the fellowship from Science and Engineering Research Board (SERB) (PDF/2018/002668).

References

[1] P. Assari, H. Adibi and M. Dehghan, *A meshless method based on the moving least squares (MLS) approximation for the numerical solution of two-dimensional nonlinear integral equations of the second kind on non-rectangular domains,* Numer. Algor (2014) 67:423–455.

[2] Z. Avazzadeh, M. Heydari, W. Chen and G.B. Loghmani, *Exponential convergence for numerical solution of integral equations using radial basis functions*, J. Appl. Math., Volume 2014, Article ID 710437, 9 pages.

[3] I. Aziz, S. Islam, and B. Sarler, *Wavelets collocation methods for the numerical solution of elliptic BV problems*, Appl. Math. Model., 37(2013), 676–694.

[4] E. Babolian, S. Bazm and P.Lima, *Numerical solution of nonlinear two-dimensional integral equations using rationalized Haar functions*, Commun. Nonlinear Sci. Numer. Simulat., 16 (2011), 116–1175.

[5] E. Babolian and F. Fattahzadeh, *Numerical solution of differential equations by using Chebyshev wavelet operational matrix of integration*, Appl. Math. Comput., 188 (2007), 417–426.

[6] E. Babolian and F. Fattahzadeh, *Numerical solution of differential equations by using Chebyshev wavelet operational matrix of integration*, Appl. Math. Comp., 188(2007), 417–426.

[7] A.H. Borzabadi and M. Heidari, *A successive iterative approach for two dimensional Volterra-Frredholm integral equations*, Iranian J. Numer. Anal. & Optim., Vol 4, No.1 (2014),pp 95–104.

[8] G. Chandhini K. S. Prashanthi and V. A. Vijesh A radial basis function method for fractional Darboux problems, Eng. Anal. Bound. Elem.,86 (2018) 1–18.

[9] Y. Changqing and H. Jianhua, *Chebyshev wavelets method for solving Bratu's problem*, Boundary value problems, 2013, article 142, 9 pages.

[10] M.H. Heydari, M.R. Hooshmandasl, F.M.M. Ghaini, *A new approach of the Chebyshev wavelets method for partial differential equations with boundary conditions of the telegraph type*, Appl. Math. Model., 38(2014), 1597–1606.

[11] S.A Hosseini, S. Shahmorad and F. Talati, *A matrix based method for two dimensional nonlinear Volterra-Fredholm integral equations*, Numer. Algor. DOI: 10.1007/s11075-014-9858-4.

[12] M. K. Jain and K. D. Sharma *Cubature method for the numerical solution of the characteristic initial value problem* $u_{xy} = f(x, y, u, u_x, u_y)$, J. Austral Math Soc., (8) 1968,355–368.

[13] R. Jiwari, *A Haar wavelet quasilinearization approach for numerical simulation of Burgers' equation*. Comput. Phys. Comm., 18(2012), 2413–2423.

[14] H. Kaur, R.C. Mittal and V. Mishra, *Haar wavelet solutions of nonlinear oscillator equations*, Appl. Math. Model., (38)2014, 4958–4971.

[15] K. H. Kumar and V. A. Vijesh, *Chebyshev wavelet quasilinearization scheme for coupled nonlinear sine-Gordon equations*, J. Comput. Nonlinear Dynam., 12(1),011018, 05 pages.

[16] F. Mirzaee and A.A. Hoseini, *A computational method based on hybrid of block-pulse functions and Taylor series for solving two-dimensional nonlinear integral equations*, Alex. Engg. J., (2014) 53, 185–190.

[17] J.S. Nadjafi, O.R.N. Samadi and E. Tohidi, *Numerical solution of two-dimensional volterra integral equations by spectral galerkin method* , J. Appl. Math. & Bio., vol.1,no.2, 2011, 159–174.

[18] S. Nemati, P.M. Lima and Y.Ordokhani, *Numerical solution of a class of two-dimensional nonlinear Volterra integral equations using Legendre polynomials*, J. Comp. Appl. Math., 242(2013) 53–69.

[19] A.Tari, M.Y. Rahimi, S. Shahmorad, F. Talati, *Solving a class of two-dimensional linear and nonlinear volterra integral equations by the differential transform method*, J. Comp. App. Math., 228(2009) 70–76.

[20] U. Lepik, *Solving PDEs with the aid of two-dimensional Haar wavelets*, Computers & Mathematics with Applications, 61(2011), 1873–1879.

[21] A. Popov, *Lobachevsky geometry and modern nonlinear problems*, Birkhäuser, 2014.

[22] V. A. Vijesh and K. H. Kumar, *Wavelet based numerical simulation of non linear Kilen/Sine gordon equation*, J. of Combinatorics, Information and System Sciences, 40 (1) (2015), 225–244.

[23] H. Zhang, Y. Chen, C. Guo and Z. Fu, *Application of radial basis function method for solving nonlinear integral equations*, J. Appl. Math., Volume 2014, Articel ID 381908, 8 pages.

Table 1: Numerical results of Example 4.1

$(\frac{1}{2^i}, \frac{1}{2^i})$	Haar[4]	Legendre[18]	Legendre[18]	CWM	CWM
i	$m = 32$	$M = 2$	$M = 3$	$N_1 = 2$	$N_1 = 3$
0	–	$1.3e^{-02}$	$1.4e^{-03}$	$7.1e^{-18}$	0.0
1	$3.2e^{-02}$	$3.6e^{-03}$	$2.8e^{-06}$	$6.1e^{-18}$	0.0
2	$1.6e^{-02}$	$4.7e^{-04}$	$1.7e^{-04}$	$4.3e^{-18}$	0.0
3	$8.5e^{-03}$	$6.1e^{-04}$	$1.3e^{-05}$	0.0	0.0
4	$4.6e^{-03}$	$6.1e^{-04}$	$3.5e^{-05}$	0.0	0.0
5	$2.6e^{-03}$	$4.1e^{-04}$	$3.2e^{-05}$	0.0	0.0
6	$1.6e^{-04}$	$2.6e^{-04}$	$1.9e^{-05}$	0.0	0.0

Table 2: Numerical results of Example 4.1

$(\frac{1}{2^i}, \frac{1}{2^i})$	Chebyshev[17]	Legendre[17]	CWM	Chebyshev[17]	Legendre[17]	CWM
i	$N = 1$	$N = 1$	$N_1 = 1$	$N = 3$	$N = 3$	$N_1 = 3$
1	$2.9e^{-01}$	$1.8e^{-01}$	$2.1e^{-10}$	$6.0e^{-10}$	$4.0e^{-10}$	0.0
2	$1.3e^{-01}$	$4.3e^{-02}$	$2.1e^{-10}$	$2.0e^{-10}$	$5.0e^{-10}$	0.0
3	$3.1e^{-02}$	$1.1e^{-01}$	$2.1e^{-10}$	$4.7e^{-10}$	$5.5e^{-10}$	0.0
4	$1.3e^{-01}$	$2.1e^{-01}$	$2.1e^{-10}$	$6.5e^{-10}$	$5.5e^{-10}$	0.0
5	$1.9e^{-01}$	$2.7e^{-01}$	$2.1e^{-10}$	$5.5e^{-10}$	$2.1e^{-10}$	0.0
6	$2.1e^{-01}$	$3.0e^{-01}$	$2.1e^{-10}$	$6.6e^{-10}$	$2.1e^{-10}$	0.0

Table 3: Numerical results of Example 4.2

(x, t)	TDDT[19]	CWM	TDDT[19]	CWM
	$N = 10$	$N_1 = 10$	$N = 12$	$N_1 = 12$
$(0.1, 0.7)$	$5.26e^{-12}$	$9.10e^{-15}$	$1.64e^{-14}$	$2.34e^{-15}$
$(0.2, 0.3)$	$1.82e^{-15}$	$3.51e^{-14}$	$1.05e^{-18}$	$2.06e^{-15}$
$(0.3, 0.9)$	$7.64e^{-10}$	$1.11e^{-13}$	$3.92e^{-12}$	$1.99e^{-15}$
$(0.4, 1.0)$	$4.37e^{-09}$	$2.70e^{-13}$	$2.77e^{-11}$	$3.33e^{-16}$
$(0.5, 0.8)$	$5.76e^{-10}$	$1.17e^{-13}$	$2.34e^{-12}$	$2.33e^{-15}$
$(0.6, 1.0)$	$9.83e^{-09}$	$5.95e^{-13}$	$6.22e^{-11}$	$1.10e^{-16}$
$(0.7, 0.6)$	$4.69e^{-11}$	$3.58e^{-13}$	$1.07e^{-13}$	$2.33e^{-15}$
$(0.8, 1.0)$	$1.75e^{-07}$	$1.00e^{-12}$	$1.11e^{-10}$	$2.22e^{-16}$
$(0.9, 0.5)$	$1.03e^{-11}$	$4.63e^{-13}$	$1.65e^{-14}$	$2.22e^{-15}$
$(1.0, 1.0)$	$2.73e^{-08}$	$1.29e^{-12}$	$1.73e^{-10}$	$3.51e^{-14}$

Table 4: Comparison of L_∞ errors of Example 4.2

N	GWF[1]	SWF[1]	n	GA[2]	MQ[2]	IQ[2]	N_1	CWM
9	$1.88e^{-02}$	$9.75e^{-03}$	4	$2.2e^{-02}$	$2.6e^{-02}$	$2.2e^{-02}$	3	$5.46e^{-03}$
25	$2.81e^{-03}$	$1.69e^{-03}$	9	$2.5e^{-04}$	$1.2e^{-04}$	$5.2e^{-04}$	5	$2.44e^{-05}$
36	$1.62e^{-03}$	$6.02e^{-04}$	16	$3.2e^{-07}$	$3.0e^{-07}$	$4.4e^{-07}$	6	$1.07e^{-06}$
49	$4.89e^{-03}$	$3.79e^{-04}$	25	$7.1e^{-08}$	$7.4e^{-08}$	$8.0e^{-08}$	8	$9.30e^{-10}$
64	$5.76e^{-03}$	$2.16e^{-04}$	36	$6.0e^{-11}$	$5.1e^{-11}$	$5.9e^{-11}$	10	$1.06e^{-12}$

Table 5: Numerical results of Example 4.3

$(\frac{1}{2^i}, \frac{1}{2^i})$	Haar[4]	HBPF[16]	CWM
i	$m = 32$	$n = 2, m = 3$	$N_1 = 8$
1	$1.4e^{-02}$	$2.2e^{-02}$	$3.9e^{-13}$
2	$7.9e^{-03}$	$6.5e^{-04}$	$4.6e^{-12}$
3	$4.1e^{-03}$	$4.1e^{-05}$	$7.9e^{-13}$
4	$2.2e^{-03}$	$2.5e^{-06}$	$6.4e^{-11}$
5	$1.2e^{-03}$	$1.6e^{-07}$	$4.6e^{-13}$
6	$9.3e^{-09}$	$9.9e^{-09}$	$2.7e^{-10}$

Table 6: Numerical results of Example 4.3

(x, t)	Standard base[11]	Legendre base[11]	Chebyshev base[11]	CWM
$N = 12$	$N = 12$	$N = 12$	$N = 12$	$N_1 = 12$
(0.1,0.1)	$6.07e^{-09}$	$4.20e^{-11}$	$3.27e^{-12}$	$1.12e^{-15}$
(0.3,0.4)	$3.72e^{-08}$	$2.47e^{-10}$	$1.80e^{-10}$	$1.35e^{-15}$
(0.7,0.6)	$1.26e^{-06}$	$6.55e^{-08}$	$5.08e^{-08}$	$1.78e^{-15}$
(1,1)	$1.12e^{-04}$	$1.11e^{-05}$	$1.69e^{-06}$	$6.44e^{-15}$

Table 7: Numerical results of Example 4.3

(x, t)	[7]	CWM
Grid Points	10000	$144(N_1 = 12)$
(0.2,0.2)	$1.722e^{-08}$	$1.24e^{-15}$
(0.4,0.4)	$2.616e^{-07}$	$1.44e^{-15}$
(0.6,0.6)	$1.338e^{-06}$	$1.61e^{-15}$
(0.8,0.8)	$4.852e^{-06}$	$2.44e^{-15}$
(1,1)	$1.571e^{-05}$	$6.44e^{-15}$

Table 8: Numerical results of Example 4.4

(x,t)	Exact Solution	RBF [8] (21×21)	Cubature [12] (20×20)	CWM(10×10)
$(0.1,0.1)$	-0.693147181	-0.693147187	-0.693147270	-0.693147181
$(0.2,0.3)$	-0.694396660	-0.694396667	-0.694397230	-0.694396660
$(0.3,0.1)$	-0.698138869	-0.698138876	-0.698139080	-0.698138869
$(0.3,0.5)$	-0.698138869	-0.698138877	-0.698140480	-0.698138869
$(0.4,0.1)$	-0.704355244	-0.704355251	-0.704355420	-0.704355244
$(0.4,0.5)$	-0.694396660	-0.694396668	-0.694399030	-0.694396660

Table 9: Numerical results of Example 4.5

(x,t)	CWM($M=6$)	CWM($M=8$)	CWM($M=10$)
$(0.1,0.1)$	0.9984	0.9984	0.9984
$(0.3,0.3)$	0.9859	0.9859	0.9859
$(0.5,0.5)$	0.9613	0.9613	0.9613
$(0.7,0.7)$	0.9254	0.9254	0.9254
$(0.9,0.9)$	0.8783	0.8783	0.8783

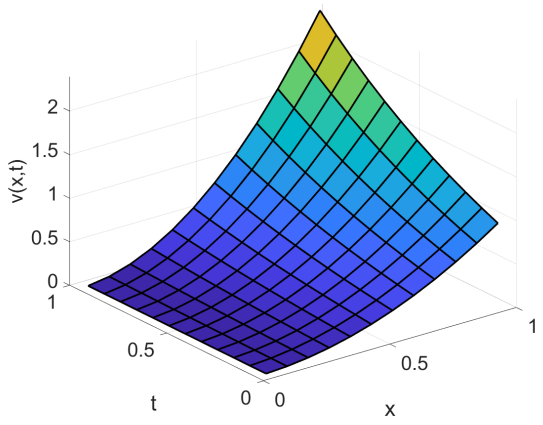

Figure 1: Numerical solution of Example 4.2

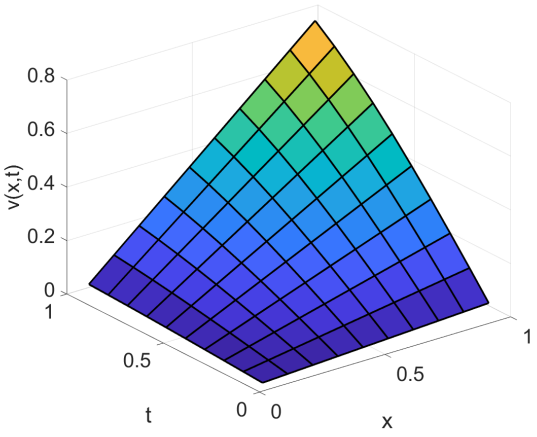

Figure 2: Numerical solution of Example 4.3

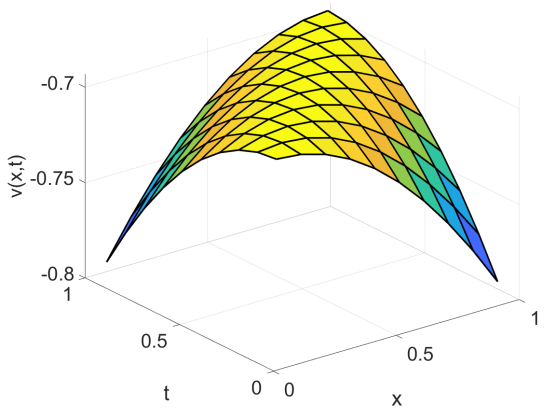

Figure 3: Numerical solution of Example 4.4

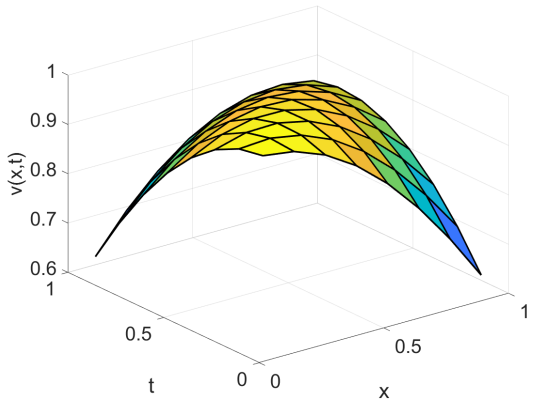

Figure 4: Numerical solution of Example 4.5

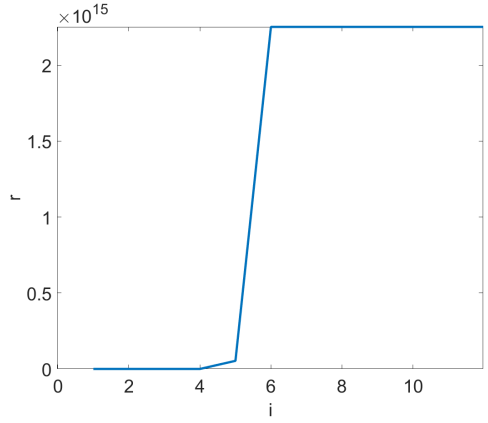

Figure 5: Plot for Example 4.1